Weierstraß-Institut
für Angewandte Analysis und Stochastik
Leibniz-Institut im Forschungsverbund Berlin e. V.

Preprint ISSN 2198-5855

Regularizing aperiodic cycles of resonant radiation in filament light bullets

Carsten Brée[1], Ihar Babushkin[2], Uwe Morgner[2], Ayhan Demircan[2]

submitted: May 5, 2017

[1] Weierstrass Institute
Mohrenstr. 39
10117 Berlin, Germany
E-Mail: carsten.bree@wias-berlin.de

[2] Institute for Quantum Optics
Leibniz Universität Hannover
Welfengarten 1
30167 Hannover, Germany
E-Mail: babushkin@iqo.uni-hannover.de
morgner@iqo.uni-hannover.de
demircan@iqo.uni-hannover.de

No. 2394
Berlin 2017

2010 *Mathematics Subject Classification.* 76B15.

2010 *Physics and Astronomy Classification Scheme.* 47.35.Bb, 47.27.Sd.

Key words and phrases. femtosecond filamentation, nonlinear optical solitons.

Edited by
Weierstraß-Institut für Angewandte Analysis und Stochastik (WIAS)
Leibniz-Institut im Forschungsverbund Berlin e. V.
Mohrenstraße 39
10117 Berlin
Germany

Fax: +49 30 20372-303
E-Mail: preprint@wias-berlin.de
World Wide Web: http://www.wias-berlin.de/

Regularizing aperiodic cycles of resonant radiation in filament light bullets

Carsten Brée, Ihar Babushkin, Uwe Morgner, Ayhan Demircan

Abstract

We demonstrate an up to now unrecognized and very effective mechanism which prevents filament collapse and allows persistent self-guiding propagation retaining larg portion of the optical energy on-axis over unexpected long distances. The key ingredient is the possibility of leaking continuously energy into the normal dispersion regime via emission of resonant radiation. The frequency of the radiation is determined by the dispersion dynamically modified by photo-generated plasma, thus allowing to excite new frequencies in the spectral ranges which are otherwise difficult to access.

Filamentation of intense femtosecond laser pulses in transparent media represents, due to the interplay of basic linear and nonlinear effects resulting from classical and quantum mechanical approaches, a physical system of interest for fundamental science as well as for a variety of applications [1, 2, 3, 4]. It is used for the investigation of , e.g., supercontinuum [5], high harmonic [6], or Terahertz generation [7], few-cycle pulse generation [9], or complex nonlinear dynamics as self-organization [8]. Analogies to other areas of physics as artificial event horizons [10] or the ubiquitous rogue wave formation [11, 12, 16] has been shown, providing an useful test for the investigation Hawking radiation [14] or predictability of extreme events [15].

The classical picture of the filamentation process which was until recently thought to be well established for nearly half of century, is based on the equilibrium between the spatial collapse due to Kerr nonlinearity and the plasma defocusing. Recently and rather unexpectedly this understanding has been questioned, especially in novel unusual regimes such as ultra-short pulses or long wavelengths. In particular, the availability of new mid-infrared ultrashort high energy laser sources led to new unusual phenomena. In Ref. [17] a superhigh power filamentation regime in air has been revealed, which is quantitatively and qualitatively different from conventional filament. The main point is that leaking energy into higher harmonics plays an important role in arresting the collapse. The fact that there are other efficient mechanisms for this besides the impact of plasma is regarded to trigger a fundamental paradigm shift in the field of extreme nonlinear optics. In Ref. [18] another new kind of significantly different filamentation process has been observed in bulk fused silica by pumping into the anomalous dispersion regime. This regime is known to exhibit much more complicated dynamics, but also to include the advantage of solitary solutions with full spatio-temporal localization and stationarity, known as light-bullets [19, 20, 21, 23, 24, 25, 26, 27]. In a filament these conditions can not be exactly fulfilled [2, 1] due to a high number of inherent perturbations [28], but the observations in Ref. [18] demonstrate unexpected long light-bullet propagation, and reveal also another interesting point. The propagation dynamics are accompanied by generation of blue shifted radiation [29], a phenomenon which is observed also under different conditions [30, 9, 31, 32, 33] even for short filament lengths.

The other, rather independent field of research which is actively developing in parallel to the filament science but with almost no overlap is one-dimensional pulse propagation in waveguides is the dynamics of solitary waves in waveguides, which appear in anomalous dispersion range and are accompanied typically by a phase-matched radiation in the normal dispersion regime [34, 35, 36]. This

DOI 10.20347/WIAS.PREPRINT.2394 Berlin 2017

so-called resonant radiation (RR) represents a central process in nonlinear waveguide optics (see Ref. [36, 37] and references within) with a remarkable rich variety of applications. There is still an increasing interest on RR, as quite recently its ability to open new routes for highly coherent light sources with unprecedented spectral range has been demonstrated [38, 39, 40, 41]. However, the investigations are mainly restricted to the one-dimensional case. The interaction with photo-generated plasma is rather unknown, but promises completely new possibilities for RR components [42].

Here we demonstrate that RR takes place in filaments in a similar way like in optical waveguides, but with even more dramatic influence on the dynamics. (i) RR provides a new and effective mechanism acting against a beam collapse and enabling stable and long on-axis channeling of optical energy, in strong difference to the conventional filamentation process. ii) The conditions for the RR generation are drastically changed by the plasma contribution, shifting the excitation peaks to positions which are otherwise not possible. This opens up completely new possibilities for exploiting RR to generate high intense and coherent radiation in different spectral ranges.

Our model [4] is based on the forward Maxwell equation of the analytical signal [43], augmented by Raman and plasma nonlinearities according to

$$\partial_z \mathcal{E}_\omega = \frac{i}{2\beta(\omega)}\Delta_\perp \mathcal{E}_\omega + i\beta(\omega)\mathcal{E}_\omega - \frac{\mu_0\omega}{2\beta(\omega)}\hat{J}$$
$$+i\frac{3\omega^2\chi^{(3)}}{8c^2\beta(\omega)}([(1-g)|\mathcal{E}|^2 + gh_{\mathrm{R}}(t) * |\mathcal{E}(t)|^2]\mathcal{E}(t))_{\omega>0} \quad (1)$$

where $\mathcal{E}_\omega$ denotes the analytic signal of the electric field $E(t)$ in the frequency domain, $*$ denotes the convolution; the free electron current $\hat{J}$ is governed by the Drude model and a rate equation for the instantaneous electron density according to the widely used tunnel ionization model of Ammosov-Delone-Krainov (ADK model)[44] for crystals, g is the fractional contribution of the Raman delayed nonlinearity, $*$ denotes the convolution integral, $h_{\mathrm{R}}(t)$ is the Raman kernel, and $\beta(\omega) = \omega n_0(\omega)/c$ is the propagation constant related to the refractive index $n_0(\omega)$ of bulk fused silica [45]. For numerical solution of Eq. 1 we use a standard de-aliased pseudospectral split-step method in combination with a 4th-order Runge-Kutta integration scheme for the higher-order nonlinearities with the implementation of an adaptive step-size control [4].

This numerical method has been shown to reproduce the filament dynamics in perfect agreement to experimental results [46]. The input pulsed beam has a center wavelength of $1900\,$nm in the anomalous dispersion regime, a Gaussian temporal profile with $t_p = 50\,$fs and a Gaussian beam waist $w_0 = 200\,\mu m$. The injected pulse has a peak power of 26 critical powers in fused silica, which amounts to an input pulse energy of $20\,\mu J$. For our chosen initial conditions, the evolution of the generated peak plasma density is shown in Fig. 1(a). We observe that the plasma density does not exceed $0.2\rho_c$, where $\rho_c = \omega_0^2 m_e \epsilon_0/q_e^2$ is the critical plasma density for which optical breakdown effects are likely to induce damage. Besides, we checked that the peak fluences do not exceed 2J/cm^2 [47, 48]. The evolution of the on-axis temporal intensity profile is depicted in Fig. 1(b). The first observation is that the pulse can maintain a high fluence along the entire propagation distance of 3.5 cm, cf. Fig. 1(c), in agreement with recent experimental and theoretical findings in Ref. [18].

Secondly, the global temporal and spectral dynamics bears significant resemblance to the periodic excitation of RR [49, 50, 51] in guided wave nonlinear optics. In the case of propagation in a fiber, a higher order soliton experiences periodic compression cycles, leading to a periodic overlap of the spectrum with a phase-matched component in the normal dispersion regime. This leads to a periodic excitation of RR. In a similar way, in our filament, the pulse maintains several temporal slices with sufficient optical power to induce aperiodic recurrent focusing/refocusing events according to the dynamic spatial replenishment model [52] (in contrast to existing periodic solutions mentioned above).

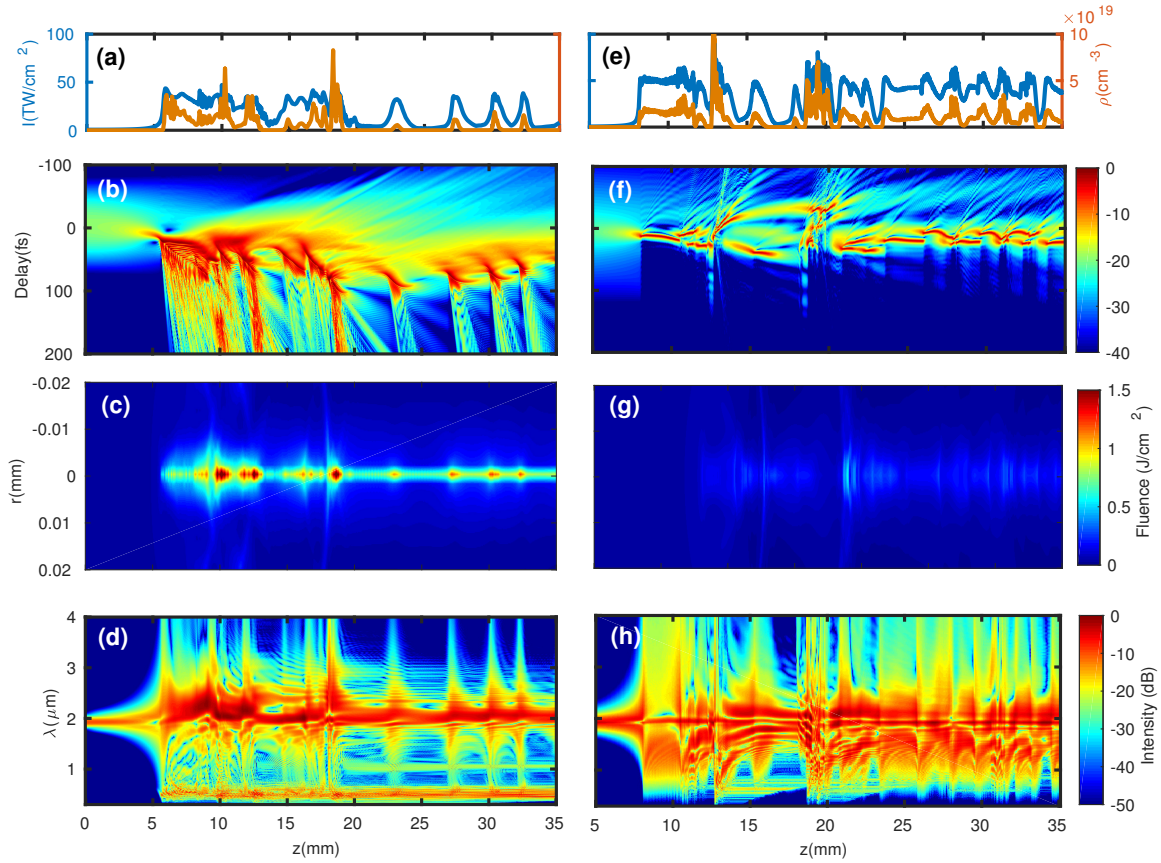

Figure 1: (a) Peak electron density (orange) and peak intensity (blue) along optical axis z for a filament seeded by a $20\,\mu$J, $1900\,$nm pulse, simulated using the full numerical model 1. (b) Corresponding aperiodic evolution of on-axis temporal intensity profile. (c) Filament fluence versus radial a longitudinal filament coordinates and (d) spectral evolution along z. Panels (e)-(h) depict the equivalent information for the same pulse, simulated using a reduced model with the dispersion including only β_2 term.

As individual time slices refocus, they propagate quasi-stationary along a distance of some millimeters and are temporally compressed and shifted towards the trailing pulse edge due to the interplay of self-steepening and anomalous dispersion [45]. Every time the corresponding spectral broadening exhibit an overlap to a phase-matched component, a pronounced emission of resonant radiation takes place [Fig. 1(d)], transferring the energy into the normally dispersive frequency domain. The corresponding resonance condition will be discussed later. In addition, upon self-focusing the pulse envelope gets strongly modulated and splits into temporal components co-propagating with the main pulse at roughly the same group velocity. This is also reminiscent of the soliton splitting dynamics induced by modulation instability (MI) [50]. The spectral evolution shown in Fig. 1(d) reveals that the emitted RR occupies multiple spectral peaks which, as z grows, evolve into a quasi-continuous spectrum of RR around the wavelength range between $\lambda = 600\,$nm and $300\,$nm. The amount of energy in the RR depends on its spectral overlap with the pump. We performed a number of simulations by varying the input parameters (power, wavelength, beam waist, pulse width) and observed this behavior over wide ranges in the parameter space, demonstrating a strong robustness rather than the necessity for a delicate choice of parameters.

To demonstrate that the emission of normally dispersive RR plays an important role in regularizing the collapse dynamics we performed additional simulations with a reduced parabolic dispersion model,

$\beta(\omega) = \beta(\omega_0) + 1/v_g(\omega - \omega_0) + 1/2\beta_2(\omega - \omega_0)^2$, where $v_g = 1/\beta_1$ is the group velocity and $\beta_2 = -810\,\mathrm{fs}^2/\mathrm{cm}$ is the GVD coefficient for silica at ω_0, respectively.

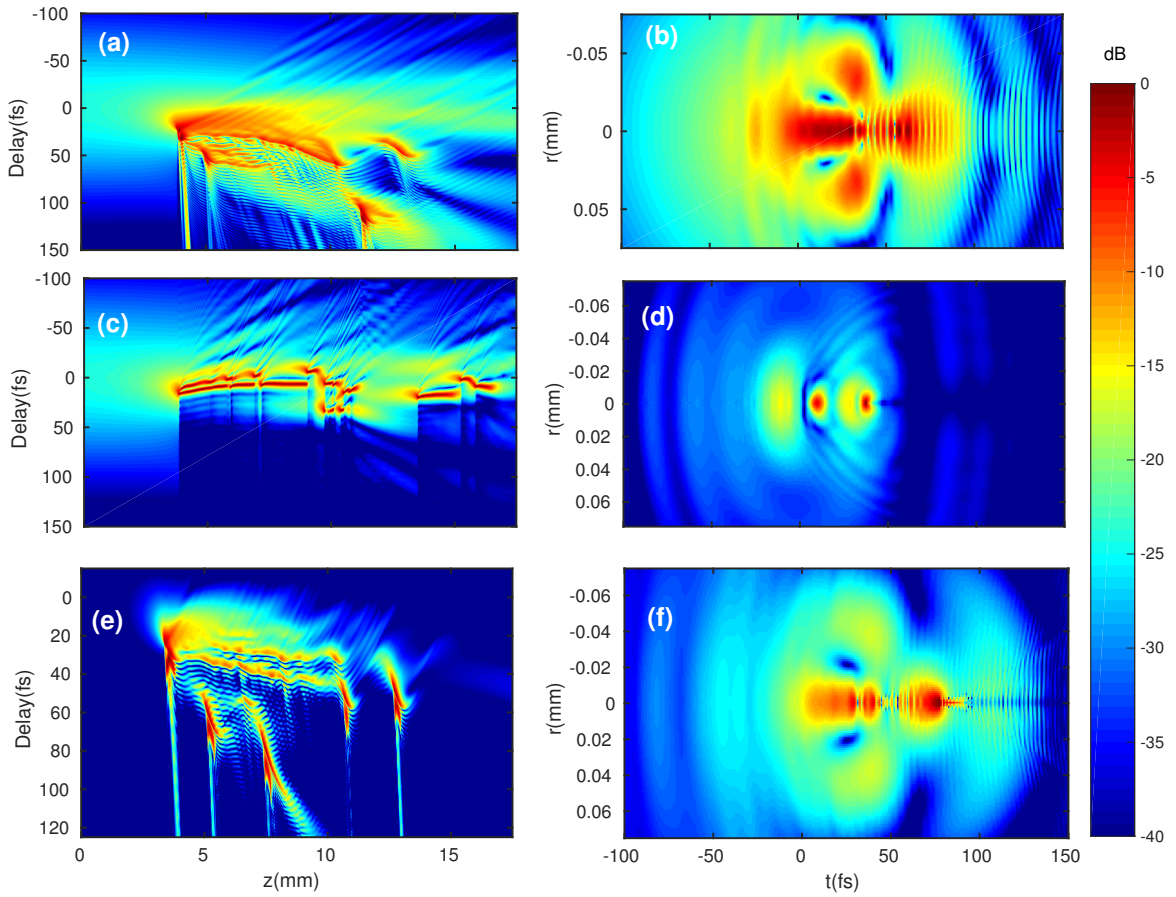

Figure 2: Pulse dynamics for lower peak power for different wavelengths and dispersion profiles. (a) On-axis temporal intensity profile for a $5.6\,\mu$J pulse at $1800\,$nm, model with full dispersion. (b) Train of light bullets at $z = 7$mm. (c),(d) The same as (a),(b), but with reduced parabolic dispersion. (e),(f) The same as (a),(b) but for $7\,\mu$J pulse at $2000\,$nm.

This choice completely eliminates the higher-order dispersion and no RR can be emitted. For the same pulse energy of $20\,\mu$J as in Figs. 1(a)-(d), peak plasma densities of 50% of the critical plasma density ρ_c are reached, which is much closer to the critical breakdown threshold than in the case of the realistic dispersion. It is necessary to mention, that we choose an example which allows a comparison between the scenarios. For higher input powers the differences become stronger, especially concerning the filament length. The corresponding evolution of the intensity, peak plasma density, on-axis temporal profile, fluence and spectrum are shown in Figs. 1(e)-(h). The overall observed dynamics are obviously different. Interestingly, in Fig. 1(f), defined light-bullets emerge exhibiting stable propagation along several millimeters, but abruptly disappear and re-appear on-axis. The strong distinctiveness of the filamentation scenario with the possibility of RR becomes evident in the evolution of the optical energy in the transverse spatial domain as shown in Fig. 1(c)and (g), for the case with and without a ZDW, respectively. With a ZDW, a huge part of the energy is retained on-axis in a stable channel along the whole filament length [Fig. 1(c)]. The observed behavior is at the first sight similar to the scenario observed in Ref. [17].

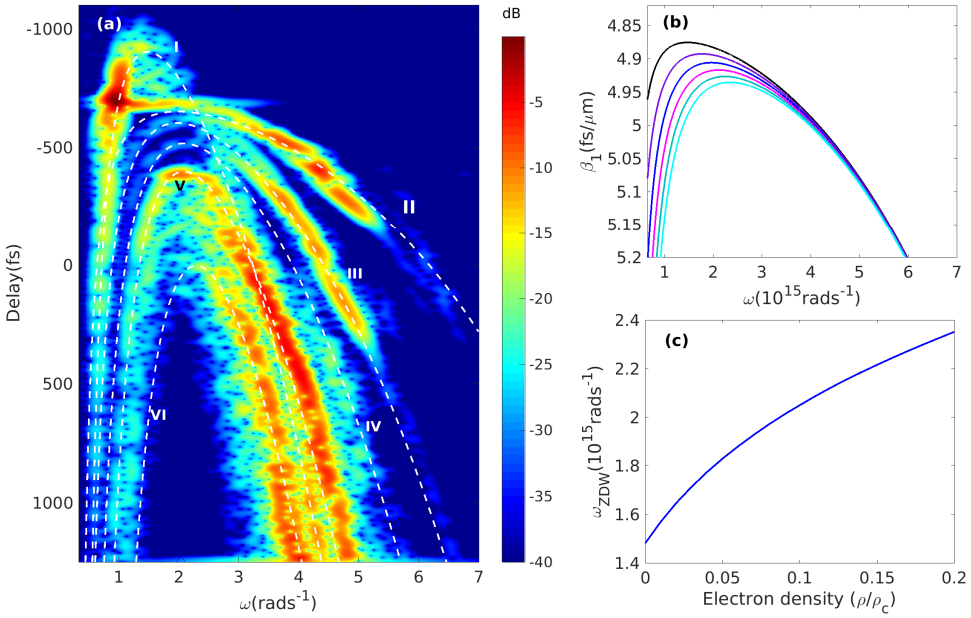

Figure 3: (color online) a) Spectrogram of an-axis temporal intensity profile at $z = 3$ cm. White dashed lines: fit according to Eq. (2) of the branches I-VI. b) Inverse group velocity for increasing electron density. (c) ZDW frequency vs. free electron density.

However, here neither shock formation nor third harmonics are required to allow the leakage of the radiation from the fundamental to another frequencies. To investigate the impact of RR generation on light-bullet formation, we repeated the same approach at low input energy (5.6 μJ, $5P_{cr}$) and center wavelength 1800 nm, with only a few focusing/refocusing events [Fig. 2(a,b)].

With the full dispersion profile, we observe the excitation of RR at approx. $z = 4, 5, 12$ mm [Fig. 2(a)], but with a relative long persistent propagation of the main on-axis part of the filament. The reduced, β_2-only model, shows a completely different behavior. Here, the initial pulse splits into two pronounced light bullets propagating stably between $z = 4 - 10$ mm [Fig. 2(c)]. Their individual trajectories appear much more stable and the individual pulse durations are much shorter than in the full-model case. In Figs. 2(b) and (d), we illustrate the spatio-temporal profiles of the emergent light bullets at $z = 7$ mm. Shifting the central wavelength to 2000nm, away from the ZDW, we expect the emission of RR to become less effective [50]. In fact, the resulting temporal evolution in Fig. 2(e,f) reveals that the filament scenario is now closer to the pure light-bullets scenario shown in Fig. 2(c,d).

To further elucidate the physical mechanisms leading to the formation of RR, we visualize the temporal dynamics of different frequency components with the XFROG technique [53] [Fig. 3(a)]. The emitted radiation is localized on several distinct branches, the dynamics of which is subject to an equation of motion governed by the inverse group velocity $k_1 = dk(\omega)/d\omega$, according to $dt(\omega)/dz = k_1(\rho(z), \omega) - 1/v_R$ where v_R is the velocity of the co-moving reference frame. Here, the dependence of k_1 on the electron density $\rho(z)$ generated at z can be derived from the Drude relation $k(\omega) = \omega/c(n_0(\omega)^2 + \omega_p^2/\omega^2)^{1/2}$ [54], where $\omega_p = \sqrt{\rho e^2/(\epsilon_0 m_e)}$ is the plasma frequency. Fig. 3(b) shows the derived $k_1 = dk(\omega)/d\omega$ curves for different ratios of ρ/ρ_c, where the black curve indicates the inverse GV of fused silica for $\rho = 0$. In fact, we find that higher electron densities shift the ZDW towards bluer frequencies, as also shown in Fig. 3(c).

Integrating the simplified evolution equation for the branches of radiation in the XFROG trace, we

obtain $t(\omega, z) = t_0(\omega) - 1/v_R(z - z_0) + \int_{z_0}^{z} dz k_1(\rho(z), \omega)$. By virtue of the first mean value theorem of integration this can be simplified to

$$t(\omega, z) = t_0(\omega) + (k_1(\rho(\xi), \omega) - \frac{1}{v_R})(z - z_0) \tag{2}$$

for some intermediate $\xi \in [z_0, z]$. In order to fit these curves to the numerically obtained XFROG trace, we assume that immediately after emission, we observe that each branch results from a burst of resonant radiation occurring at a particular coordinate tuple (t_0, z_0) By close inspection of both Fig. 1(b) and the evolution of the XFROG trace versus z, we find that the branches I-VI correspond to six dominant radiation bursts located at $(z_0\,[\text{mm}], t_0\,[\text{fs}])$=(27.2,74), (22.8,83), (18.2,83.6), (15.7,60.5), (12.2,60.83), (9.1,75.8). Therefore, the only remaining free parameter in Eq. 2 is the intermediate electron density $\rho(\xi)$, and the best fit to the XFROG trace can be obtained by choosing $\rho(\xi) = [0.1,\, 0.04,\, 0.7,\, 0.15,\, 0.3,\, 0.6] \times 10^{20}\,\text{cm}^{-3}$ for the branches I to VI, respectively. These values are close to the actual electron densities generated at the radiation bursts [cf. 1(a) brown line]. Furthermore, our analysis confirms that the dispersion of the blue spectral wings is strongly affected by plasma-induced modifications of the refractive index.

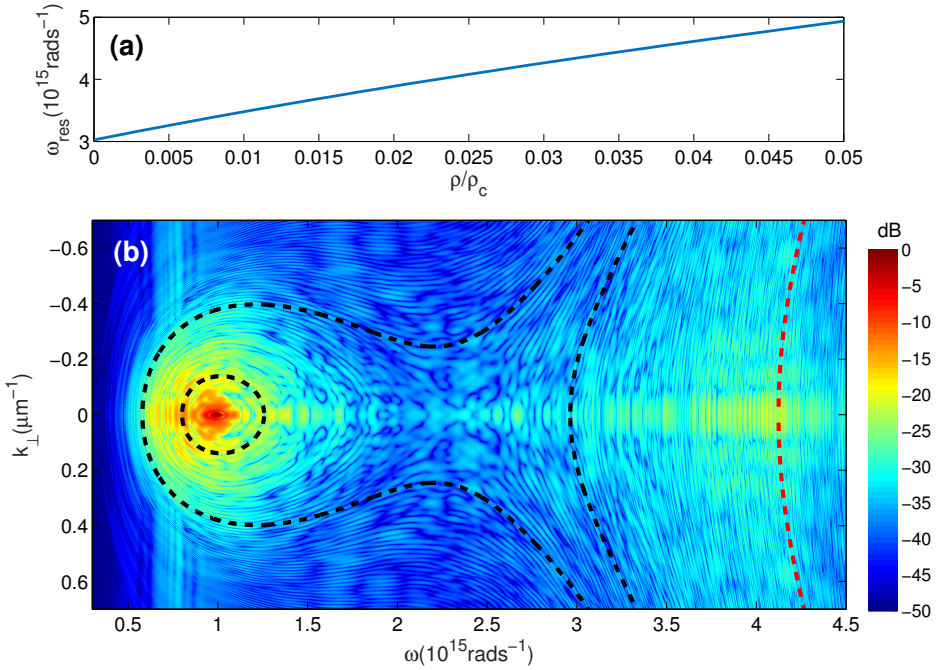

Figure 4: (color online) a) Frequency of RR according to (Eq. 3) vs electron density, for $\Delta k = 0$ and $k_\perp = 0$. b) Fourier-Hankel transform of $\mathcal{E}(r, t)$. Black dashed lines: MI gain curves for $\rho = 0$ and $\Delta k = 20\text{cm}^{-1}$ and 150cm^{-1}. Blue dashed line: Curve for electron density $8.3 \times 10^{18}\text{cm}^{-3}$ and $\Delta k = 20\text{cm}^{-1}$.

For a further analysis of the impact of the plasma GVD on the RR, we have to consider the spatio-temporal MI which acts on the filamenting pulses. According to [45], curves of constant exponential MI gain in the $(k_\perp, \omega)$-plane are defined by

$$k^2(\omega) - k_\perp^2 - (k_0 - \Delta k + (\omega - \omega_0)/v_g)^2 = 0 \tag{3}$$

where k_0 and $k_\perp$ denote the wave vector at the center frequency and the transverse wave vector component, respectively, v_g is the corresponding group velocity, and Δk the phase mismatch. The impact of plasma dispersion on $k(\omega)$ is modelled according to [54]. Solving Eq. (3) for $k_\perp = 0$, the RR frequency exhibits a considerable blueshift for increasing electron density, as shown in Fig. 4a). To compare the predictions of Eq. (3) with the simulation results corresponding to Fig. 1, in Fig. 4(b) we show the Fourier-Hankel transform of the electric field $\mathcal{E}(r,t)$ at $z = 19.2\,\text{mm}$. In the anomalous dispersion regime, the impact of spatio-temporal MI is seen from the annular structures around ω_0 and $k_\perp = 0$. In the normal dispersion regime, the resonant radiation occupies hyperbola in the $(k_\perp, \omega)$-plane.

The solutions of Eq. (3) for vanishing electron densities are shown as black-dashed lines and are in reasonable agreement with the energy distribution of the simulated pulse. Nevertheless, we find that RR also occupies hyperbola originating at considerably higher frequencies at about 4PHz than predicted by Eq. (3) with $\rho = 0$. In fact, this part of the spectrum can be attributed to blueshifted RR due to the plasma-modification of $k(\omega)$. This is shown by the blue-dashed curve in Fig. 4(b), which represents a solution of Eq. (3) with $\rho = 8.3 \times 10^{18}\text{cm}^{-3}$, the peak electron density in the simulations.

In conclusion, we demonstrated that resonant radiation generation enables relatively long filaments by a new type of collapse-arresting mechanism. Besides the qualitative different self-guiding mechanism also the properties of the filament are quite distinctive to conventional filamentation. Furthermore, we provided clear evidence, that the impact of plasma via its modifying impact on the GVD leads to the excitation of new RR frequencies in otherwise inaccessible and over wide spectral ranges. The whole process does not only provide a new concept for light-bullet generation, but also opens up new routes for tailoring light on demand.

References

[1] L. Bergé, S. Skupin, R. Nuter, J. Kasparian, J. P. Wolf, Rep. Prog. Phys. **70**, 1633 (2007).

[2] A. Couairon, and A. Mysyrowicz, Phys. Rep. **441**, 47-189 (2007).

[3] D. Mihalache, Rom. J. Phys. **59**, 295 (2016)

[4] C. Brée, Nonlinear optics in the filament regime, Springer-Verlag, Berlin, Heidelberg, 1st edn. (2012).

[5] V. P. Kandidov, O. G. Kosareva, I. S. Golubtsov, W. Liu, A. Becker, N. Akozbek, C. M. Bowden, and S. L. Chin, Appl. Phys. B **77**, 149-165 (2003).

[6] C. M. Heyl, H. Coudert-Alteirac, M. Miranda, M. Louisy, K. Kovacs, V. Tosa, E. Balogh, K. Varju, A. L'Huillier, A. Couairon, and C. L. Arnold, Optica **3**, 75-81 (2016).

[7] L. Berge, S. Skupin, C. Köhler, I. Babushkin, and J. Herrmann, Phys. Rev. Lett. 110, 073901 (2013).

[8] F. Maucher, T. Pohl, S. Skupin, and W. Krolikowski, Phys. Rev. Lett. **116**, 163902 (2016).

[9] F. Silva, D. R. Austin, A. Thai, M. Baudisch, M. Hemmer, D. Faccio, A. Couairon, and J. Biegert, Nat. Comm. **3**, 807 (2012).

[10] D. Faccio, S. Cacciatori, V. Gorini, V. G. Sala, A. Averchi, A. Lotti, M. Kolesik and J. V. Moloney, Europhys. Lett. **89**, 34004 (2010).

[11] J. Kasparian, P. Bejot, J.-P. Wolf, and J. M. Dudley, Opt. Express **17**, 12070-12075 (2009).

[12] S. Birkholz, E. T. J. Nibbering, C. Bree, S. Skupin, A. Demircan, G. Genty, and G. Steinmeyer, Phys. Rev. Lett. **111**, 243903 (2013).

[13] T. Roger, D. Majus, G. Tamosauskas, P. Panagiotopoulos, M. Kolesik, G. Genty, I. Grazuleviciute, A. Dubietis, and D. Faccio, Phys. Rev. A **90**, 033816 (2014).

[14] F. Belgiorno, S. L. Cacciatori, M. Clerici, V. Gorini, G. Ortenzi, L. Rizzi, E. Rubino, V. G. Sala, and D. Faccio, Phys. Rev. Lett. 105, 203901 (2010).

[15] S. Birkholz, C. Bree, A. Demircan, and G. Steinmeyer, Phys. Rev. Lett. **114**, 213901 (2015).

[16] T. Roger, D. Majus, G. Tamosauskas, P. Panagiotopoulos, M. Kolesik, G. Genty, I. Grazuleviciute, A. Dubietis, and D. Faccio, Phys. Rev. A **90**, 033816 (2014).

[17] P. Panagiotopoulos, P. Whalen, M. Kolesik, and J. V. Moloney, Nature Photonics **9**, 543 (2015).

[18] M. Durand, A. Jarnac, A. Houard, Y. Liu, S. Grabielle, N. Forget, A. Durécu, A. Couairon and A. Mysyrowicz, Phys. Rev. Lett. **110**, 115003 (2013).

[19] Y. Silberberg, Opt. Lett. **15**, 1282 (1990).

[20] B. A. Malomed, D. Mihalache, F. Wise, and L. Torner, J. Opt. B **7**, R53 (2005).

[21] H. Leblond and D. Mihalache, Phys. Rep. **523**, 61 (2013).

[22] B. Malomed, L. Torner, F. Wise, and D. Mihalache, J. Phys. B: At. Mol. Opt. Phys. **49**, 170502 (2016).

[23] K. E. Strecker et al., Nature **417**, 150 (2002).

[24] L. Berge, Phys. Rep. **303**, 259 (1998).

[25] D. Majus, G. Tamosauskas, I. Grazuleviciute, N. Garejev, A. Lotti, A. Couairon, D. Faccio, and A. Dubietis, Phys. Rev. Lett. **112**,193901 (2014).

[26] S- V. Chekalin and A. E. Dokukina and A. E. Dormidonov, V. O. Kompanets, E. O. Smetanina, and V. P. Kandidov, J. Phys. B **48**, 094008 (2015).

[27] E. O. Smetanina, V. O. Kompanets, A. E. Dormidonov, S. V. Chekalin and V. P. Kandidov, Laser Phys. Lett. **10**, 105401 (2013).

[28] M. Trippenbach and Y. B. Band, Phys. Rev. A **57**, 4791 (1998); S. Skupin and L. Bergé, Physica D **220**, 14 (2006); J. Liu, R. Li, and Z. Xu, Phys. Rev. A **74**, 043801 (2006); L. Bergé and S. Skupin, Phys. Rev. E **71**, 065601(R) (2005); M. Hemmer, M. Baudisch, A. Thai, A. Couairon, and J. Biegert, Opt. Express **21**, 28095 (2013), B. Shim, S. E. Schrauth, and A. L. Gaeta, Opt. Express **19**, 9118 (2011).

[29] M. Durand, K. Lim, V. Jukna, E. McKee, M. Baudelet, A. Houard, M. Richardson, A. Mysyrowicz, and A. Couairon, Phys. Rev. A **87**, 043820 (2013).

[30] A. Saliminia, S. L. Chin, and R. Vallée, Opt. Express **13**, 5731 (2005).

[31] D. Faccio, A. Averchi, A. Couairon, A. Dubietis, R. Piskarskas, A. Matijosius, F. Bragheri, M. A. Porras, A. Piskarskas, and P. Di Trapani, Phys. Rev. E **74**, 047603 (2006).

[32] E. O. Smetanina, V. O. Kompanets, S. V. Chekalin, A. E. Dormidonov, and V. P. Kandidov, Opt. Lett. **38**, 16 (2013).

[33] A. E. Dormidonov, V. O. Kompanets, S V. Chekalin, V. P. Kandidov, Opt. Express **23**, 29202 (2015).

[34] N. Akhmediev, and M. Karlsson, Phys. Rev. A **51**, 2602 (1995).

[35] A.V. Husakou and J. Herrmann, Phys. Rev. Lett. **87**, 203901 (2001).

[36] D.V. Skryabin and A.V. Gorbach, Rev. Mod. Phys. **82**, 1287 (2010).

[37] J. M. Dudley and J. R. Taylor, Nat. Photon. **3**, 85 (2009).

[38] L. G. Wright, S. Wabnitz, D. N. Christodoulides, and F. W. Wise Phys. Rev. Lett. **115**, 223902 (2015).

[39] I. Babushkin, A. Tajalli, H. Sayinc, U. Morgner, G. Steinmeyer, and A. Demircan, Light Sci Appl.**6**, e16218 (2017).

[40] V. Brasch, M. Geiselmann, T. Herr, G. Lihachev, M. H. P. Pfeiffer, M. L. Gorodetsky, T. J. Kippenberg, Science 351, 357 (2015).

[41] C. R. Loures, T. Roger, D. Faccio, F. Biancalana, Phys. Rev. Lett. **118**, 043902 (2017).

[42] D. Novoa, M. Cassataro, J. C. Travers, and P. St. J. Russell Phys. Rev. Lett. **115**, 033901 (2015).

[43] Sh. Amiranashvili and A. Demircan, Phys. Rev. A. **82**, 013812 (2010); Adv. Opt. Tech. **2011**, 989515 (2011).

[44] M. V. Ammosov, N. B. Delone, V. P. and Krainov, Sov. Phys. JETP **64**, 1191 (1968).

[45] L. Bergé, S. Mauger and S. Skupin, Phys. Rev. A **81**, 013817 (2010).

[46] M. Kretschmar, C. Brée, T. Nagy, A. Demircan, H. G. Kurz, U. Morgner, M. Kovacev Opt. Express **22**, 22905 (2014).

[47] D. Rayner, A. Naumov and P. Corkum, Opt. Express **13**, 3208 (2005).

[48] J. R. Peñano, P. Sprangle, B. Hafizi, W. Manheimer and A. Zigler, Phys. Rev. E **72**, 1 (2005).

[49] I. Cristiani, R. Tediosi, L. Tartara and V. Degiorgio, Opt. Express **12**, 124 (2004).

[50] A. Demircan and U. Bandelow, Appl. Phys. B **86**, 31 (2007).

[51] R. Driben, A. V. Yulin and A. Efimov, Opt. Express **23**, 19112 (2015).

[52] M. Mlejnek, E. M. Wright and J. V. Moloney, Opt. Lett. **23**, 382 (1998).

[53] S. Linden, H. Giessen and J. Kuhl, physica status solidi (b) **206**, 119 (1998).

[54] I. Koprinkov, Appl. Phys. B **79**, 359 (2004).